Research Square

Preprints are preliminary reports that have not undergone peer review.
They should not be considered conclusive, used to inform clinical practice,
or referenced by the media as validated information.

Microstructure and Mechanical Properties of Si_3N_4/Cu Joints Brazed Using CuSnTi and In-Alloyed CuSnTi Active Brazing Fillers in Vacuum

Furui Xu
Hebei University of Technology
Lutong Qie
Hebei University of Technology
Weibing Guo
gwbingo@163.com
Hebei University of Technology
Zongyang Dou
Hebei University of Technology
Haitao Xue
Hebei University of Technology
Cuixin Chen
Hebei University of Technology

Research Article

Keywords: CuSnTi, Interface structure, TiN, Ti5Si3, Peel strength

Posted Date: May 18th, 2026

DOI: https://doi.org/10.21203/rs.3.rs-9563636/v1

License: This work is licensed under a Creative Commons Attribution 4.0 International License.
Read Full License

Additional Declarations: No competing interests reported.

Version of Record: A version of this preprint was published at Journal of Materials Science: Materials in Electronics on June 17th, 2026. See the published version at https://doi.org/10.1007/s10854-026-17799-4.

Microstructure and Mechanical Properties of Si_3N_4/Cu Joints Brazed Using CuSnTi and In-Alloyed CuSnTi Active Brazing Fillers in Vacuum

Furui Xu [a,b], Lutong Qie [a,b], Weibing Guo [a,b*], Zongyang Dou [a,b], Haitao Xue [a,b*], Cuixin Chen [a,b]

a School of Materials Science and Engineering, Hebei University of Technology, Tianjin 300130, China

b State Key Laboratory of High Performance Roll Materials and Composite Forming, Hebei University of Technology, Tianjin 300130, China

** Correspondence:*

Weibing Guo, School of Materials Science and Engineering, Hebei University of Technology, Tianjin 300130, China.

Email: gwbingo@163.com

Haitao Xue, School of Materials Science and Engineering, Hebei University of Technology, Tianjin 300130, China.

Email: xuehaitao@126.com

Abstract:

Si_3N_4-based copper-clad laminates (CCLs) possess outstanding insulation, thermal conductivity and thermal shock resistance, with wide applications in electronic devices. Nevertheless, Si_3N_4/Cu joints suffer from large residual stress and high fabrication cost, and heat accumulation easily induces module failure under high chip power density. Herein, low-cost CuSnTi filler was adopted to braze Si_3N_4 ceramic and Cu, and the influence of brazing temperature on interfacial microstructure and mechanical performance was investigated. The CuSnTi filler exhibits good wettability on Si_3N_4,

and the joint interfacial structure is Si_3N_4/TiN+Ti_5Si_3+Cu(s, s)+CuTi+$CuTi_2$+Sn_3Ti_5/Cu. With temperature rising from 850 °C to 1000 °C, joint peel strength increases steadily and peaks at 32.1 N/mm at 1000 °C, owing to the thickened TiN layer and residual stress relaxation of Ti_5Si_3. To lower the brazing temperature, 10 wt.% In was added into CuSnTi to fabricate composite filler. The optimized temperature drops to 850 °C while peel strength remains 20.58 N/mm. In dissolves in Cu matrix to reduce melting point and improve filler fluidity, and the interfacial microstructure is well maintained. This work provides a low-cost, low-temperature and silver-free brazing route for Si_3N_4-based CCLs with promising engineering application value.

Keywords: CuSnTi, Interface structure, TiN, Ti_5Si_3, Peel strength

1. Introduction

Si_3N_4 ceramic is regarded as the core material for ceramic copper-clad laminates (CCLs) used in power electronic devices, owing to its high thermal conductivity, excellent electrical insulation, remarkable thermal shock resistance and chemical stability [1-3]. Si_3N_4-based CCLs fabricated by combining Si_3N_4 ceramic with high-conductivity Cu foil can effectively solve the heat dissipation and insulation bottlenecks of high-power chips, which is essential for the miniaturization and high integration of electronic devices [4-7]. As a key technology for dissimilar material joining, brazing presents obvious advantages over diffusion bonding, such as simple sample preparation, convenient operation and high production efficiency, making it the most widely used technique for the industrial fabrication of Si_3N_4/Cu joints [8,9].

However, two critical problems still restrict the practical application of Si_3N_4/Cu brazed joints. On the one hand, the chemically inert surface of Si_3N_4 ceramic leads to poor wettability of most conventional brazing fillers, whereas satisfactory wettability is a prerequisite for reliable metallurgical bonding. On the other hand, the large mismatch in coefficients of thermal expansion (CTE) between Si_3N_4 (3.2×10^{-6} K^{-1}) and Cu (17.0×10^{-6} K^{-1}) inevitably generates high residual stress in the joint during cooling, which degrades the joint reliability and even causes substrate cracking in severe cases [10-12].

Ag-based brazing fillers including AgCuTi and AgCuInTi have been widely applied in industrial production owing to their superior wettability on ceramics and favorable bonding strength with metals [13-15]. Tang et al. [16] used Ag-Cu-TiH_2 brazing filler metal to realize the active brazing connection of Si_3N_4 ceramic and oxygen-free copper foil at 875 °C for 0.5 h. Ti reacts with Si_3N_4 in the brazing filler metal to form TiN+Ti_5Si_3 interface reaction layer. When the content of TiH_2 is 5 wt.%, the peel strength of the joint is the best, reaching 25.1 N/mm. The evolution of the interface microstructure directly determines the fracture mechanism and mechanical properties of the joint. Nevertheless, the high cost of noble metal Ag and the Ag electromigration effect, which induces the long-term reliability degradation of CCLs, have motivated researchers to develop low-cost silver-free or low-silver brazing fillers. Cu-based active brazing fillers have attracted extensive attention as promising candidates for ceramic brazing, due to their low cost, high interfacial reactivity and

excellent thermal conductivity, which match the thermal management requirements of electronic device substrates [17-19].

Previous studies have verified the feasibility of Cu-based active fillers for Si_3N_4 brazing. Naka et al. [20] studied the wetting angle evolution of Cu-Ti and Cu-Zr alloys on Si_3N_4 ceramic with temperature and time via high-speed photography, and found that Cu-30Ti (at.%) alloy formed a TiN reaction layer thicker than 10 μm on Si_3N_4 at 1100 °C for 30 min, achieving a low wetting angle of only 8°. Wang et al. [21] investigated the wettability of CuZrTi fillers with different Ti contents on Si_3N_4 ceramic using the sessile drop method, and confirmed that the active Ti element dramatically reduced the wetting angle from 149° for pure Cu to 4° for Cu-8.6Zr-20Ti (at.%), which was ascribed to the formation of Ti-containing reaction products and the adsorption of Ti atoms at the interface. Although Cu-Ti binary fillers have been used for Si_3N_4 brazing, their excessively high brazing temperature (above 1100 °C) limits their industrial application [22]. The addition of Sn can effectively decrease the melting point of CuTi-based fillers, and CuSnTi fillers have been widely used in the joining of diamond and other materials owing to their cost effectiveness and moderate brazing temperature (around 900 °C) [23-25]. However, systematic research on the vacuum brazing of Si_3N_4/Cu joints using CuSnTi filler is still insufficient. In particular, the relationship among brazing temperature, interfacial microstructure evolution and mechanical properties of the joints has not been clearly revealed. In addition, the introduction of low-melting-point elements is an effective strategy to further lower the brazing temperature of Cu-based fillers. Indium (In), with a melting point of 156.6 °C, has been

adopted to modify Ag-based and Cu-based fillers to improve their fluidity and reduce the brazing temperature [26,27]. However, the mechanism by which In addition influences the melting point, fluidity and interfacial reaction behavior during brazing remains unclear, and the effect of In on the mechanical properties of Si_3N_4/Cu joints needs to be further explored.

Therefore, in this work, CuSnTi active brazing filler was employed to prepare Si_3N_4/Cu joints in vacuum. The wettability of CuSnTi filler on Si_3N_4 ceramic, the interfacial microstructure evolution of Si_3N_4/Cu joints, and the effect of brazing temperature (850-1000 °C) on the peel strength were systematically studied. Furthermore, 10 wt.% In was added into CuSnTi filler to prepare a novel CuInSnTi composite filler, and the influences of In addition on the brazing behavior, interfacial microstructure and mechanical properties of Si_3N_4/Cu joints were investigated, aiming to develop a low-temperature and silver-free brazing route.

2. Experimental procedure

The ceramic substrate employed in this work was hot-pressed Si_3N_4 ceramic supplied by Fuzhou Kunpeng Optoelectronic Technology Co. Ltd., with a thermal conductivity of 80 $W \cdot m^{-1} \cdot K^{-1}$. The Si_3N_4 ceramics were prepared into two dimensions: 20 mm×20 mm×0.5 mm and 10 mm×30 mm×2 mm. Oxygen-free copper (OFC) plates with a purity higher than 99.9% were provided by Dongguan Tongda Metal Materials Co., Ltd., with thicknesses of 0.5 mm and 0.3 mm, respectively. The copper plates were cut into dimensions of 10 mm×10 mm×0.3 mm (for microstructure characterization) and 6 mm×100 mm×0.5 mm (for mechanical property tests) using a wire electrical

discharge machine (WEDM), as illustrated in Fig.1a. All substrates were first ground with 2000# SiC abrasive paper, and then further polished with a wool polishing wheel mounted on a hand-held drill. Subsequently, the polished substrates were ultrasonically cleaned in anhydrous ethanol for more than 15 min. The brazing filler powder was mixed with an organic solvent to form brazing paste, which was then coated onto the substrate surfaces through a 100-mesh screen, as displayed in Fig.1a. After that, the substrates were assembled into a sandwich structure. Fig.1b shows the schematic of the sample for microstructure observation, and Fig.1c presents the schematic of the sample for mechanical property tests.

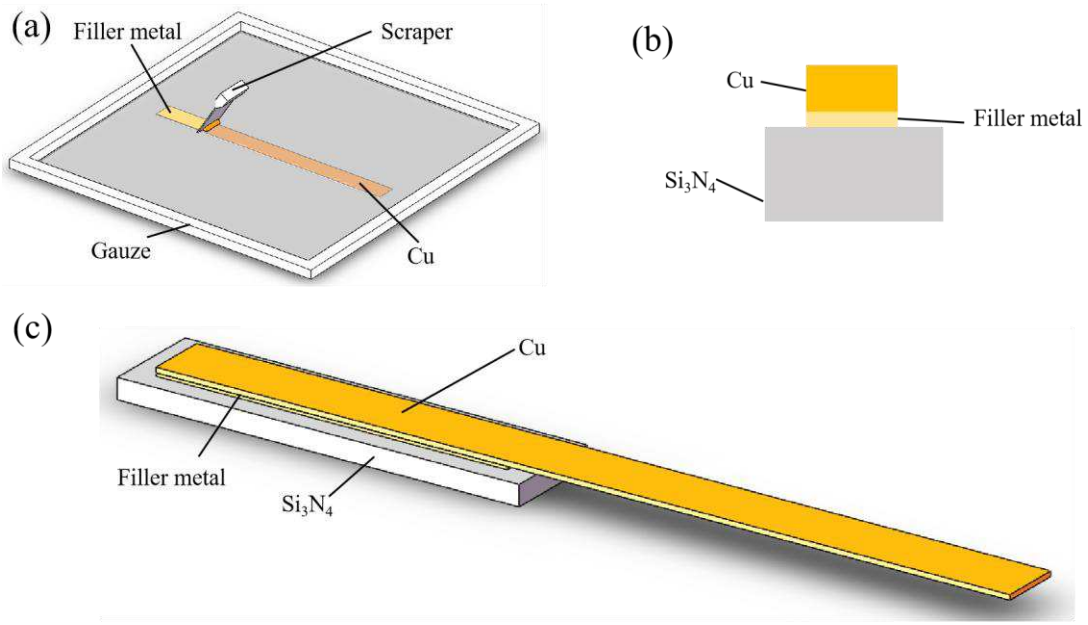


Fig.1 Diagram of Sample Preparation: (a) filler coating; (b-c) sample assembly.

The CuSnTi brazing filler metal employed in this study was supplied by Changsha Tianjiu Metal Materials Co., Ltd. The powder had a particle size of 50 μm, with a nominal composition of 20 wt.% Sn and 10 wt.% Ti. Meanwhile, 10 wt.% commercial In powder with a particle size of 38 μm was added to fabricate the CuInSnTi composite

brazing filler. The mixed powder was blended in a V-type powder mixer at 30 rpm for 48 h. The assembled samples were placed into a QVDF-200 vacuum brazing furnace, with a ultimate vacuum level of 8×10^{-4} Pa. During heating, the vacuum was maintained at $(4\text{-}8)\times10^{-3}$ Pa, and the temperature control accuracy was ±5 °C, satisfying the experimental requirements. The samples were heated to 600 °C at a rate of 15 °C/min and held for 10 min, then further heated to the target brazing temperature at 5 °C/min. A constant pressure of 0.2 MPa was applied to the samples during brazing.

Microstructure characterization was carried out using a field emission scanning electron microscope (FE-SEM, JSM-7100F) equipped with an energy dispersive spectrometer (EDS, EDAX Genesis2000), as well as an electron probe microanalyzer (EPMA, JXA-8530F). Phase identification was performed on the flat fracture surfaces after peeling tests by an X-ray diffractometer (XRD, Bruker D8 Discover) with Cu-Kα radiation. To quantitatively evaluate the bonding strength between Si_3N_4 ceramic and Cu foil, 90° peel strength was measured using a universal mechanical testing machine (AGS-XD50kN) with the custom fixture shown in Fig.2. During the test, the Cu strip was peeled from the ceramic substrate at a 90° angle around a rigid shaft. The peeling speed was set at 50 mm/min, with a peeling angle tolerance of ±5° and a peeling length no less than 30 mm. The load–displacement curve was recorded automatically, and the average peel force was obtained from the stable plateau region of the curve. To ensure the reliability of results, three parallel tests were carried out for each condition, and the average value was adopted. The peel strength (P_s, N/mm) was calculated by Equation

(1), where F_p is the average peel force (N), and l_c is the width of the Cu foil (mm, fixed at 6 mm in this work).

$$P_s = \frac{F_p}{l_c} \quad (1)$$

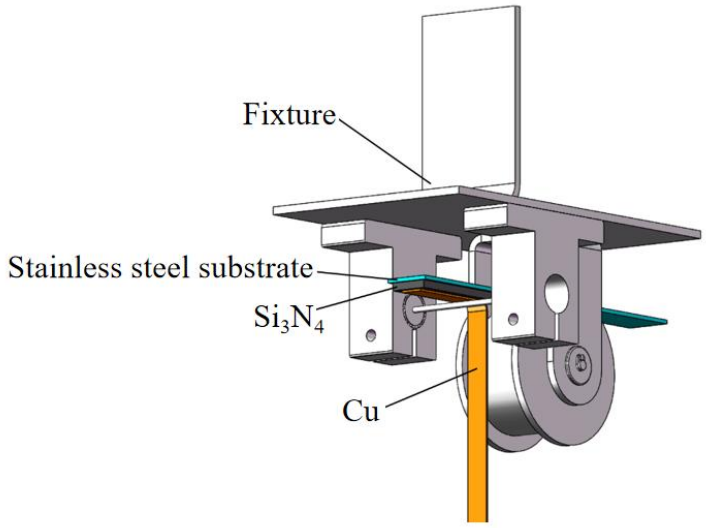


Fig.2 Fixture for Peeling strength testing.

3. Results and Discussion

3.1 Microstructure of Cu/CuSnTi/Si_3N_4 joint interface

Although extensive studies have been conducted on the wettability and bonding performance of CuSnTi brazing fillers on diamond substrates, research on their application in Si_3N_4 ceramic brazing remains relatively limited. Superior wettability of liquid brazing alloys on ceramic surfaces is a prerequisite for achieving reliable metallurgical bonding. Accordingly, the wetting behavior of CuSnTi brazing filler on Si_3N_4 ceramic was first examined in this work. Fig.3 presents the variation in the wetting angle of the CuSnTi filler on Si_3N_4 ceramic at different brazing temperatures. The filler exhibits satisfactory wettability, and the wetting angle gradually decreases with increasing brazing temperature. At 900 °C, the wetting angle is reduced to below 20°, reaching a value of 19.4°.

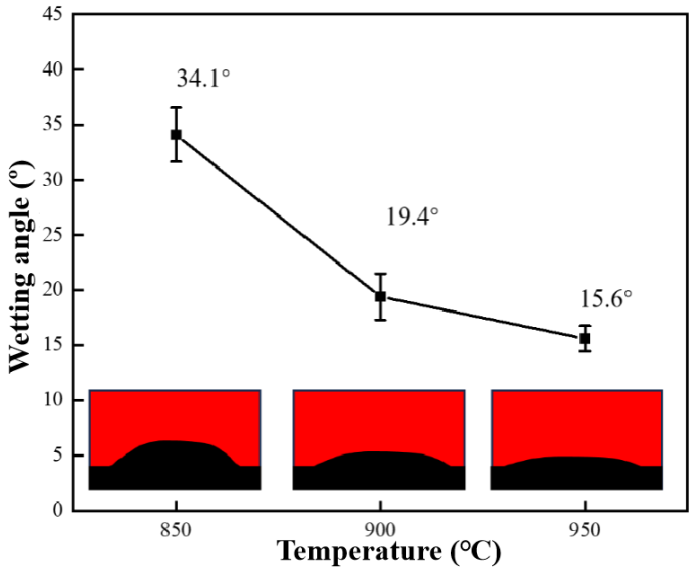


Fig.3 Change in wetting angle of CuSnTi brazing filler metal on Si_3N_4 ceramic surface.

Figure 4 shows the interfacial microstructure of the Si_3N_4/CuSnTi/Cu joint brazed at 900 °C for 20 min. As presented in Fig.4a, the joint is well bonded without obvious defects such as voids or cracks. At elevated temperatures, interdiffusion occurs between the Cu substrate and the liquid brazing alloy, leading to the blurring and disappearance of the Cu/brazing layer interface. A higher-magnification image of the joint zone (Fig.4b) displays a dominant light gray matrix phase A, a small amount of white phase B, and dark gray blocky phase C. Further magnification of the ceramic-side reaction layer (Fig.4c) reveals hexagonal black blocky phase D, black dot-like phase F within the brazing seam, and a distinct reaction layer phase E at the ceramic interface.

To identify the constituent phases in the joint, quantitative compositional analysis was performed on phases A-E using EDS, and elemental mapping was conducted via EPMA. The corresponding results are summarized in Table 1 and Fig.5, respectively. Phase A is composed of 95.80 at.% Cu, with contrast consistent with the Cu substrate, indicating that it is a Cu-based solid solution (Cu(s，s)). Phase B mainly consists of

26.78 at.% Sn, 14.70 at.% Cu, and 55.43 at.% Ti. Combined with the uniform distribution of Sn and Ti in Fig.5, phase B is confirmed to be Sn_3Ti_5. Phase C is primarily composed of Cu and Ti with an atomic ratio close to 1:1. As observed in Fig.5a, b, and d, the dark gray phases near the ceramic and the dendritic dark gray phases in the brazing seam are enriched in Cu and Ti. Thus, the Cu-Ti intermetallic compound CuTi is formed by the reaction between Ti and Cu solid solution. Phase D exhibits a regular hexagonal morphology and is mainly composed of Ti and Si. As reported in the literature [28,29], Ti and Si can react to form various titanium silicides including TiSi, Ti_5Si_3, and $TiSi_2$. At high temperatures, the Gibbs free energies of formation for all three phases are negative, while that of Ti_5Si_3 is the most negative, suggesting the highest formation priority. Moreover, the atomic ratio of Ti to Si in phase D is approximately 5:3, consistent with Ti_5Si_3 (Equation 2). Therefore, phase D is determined to be Ti_5Si_3. Phase E contains 35.98 at.% Ti and 33.96 at.% N, verifying it as the TiN interfacial reaction layer generated by the reaction between active Ti and Si_3N_4 ceramic (Equation 3) [30,31].The EDS results of the black phase at point F show 23.88 at.% Ti and 73.18 at.% Cu. Due to the small size of this phase, large errors may exist in the EDS quantification. Accordingly, it is deduced that, in addition to a large amount of CuTi, other Cu-Ti intermetallic compounds such as $CuTi_2$ may also precipitate in the joint.

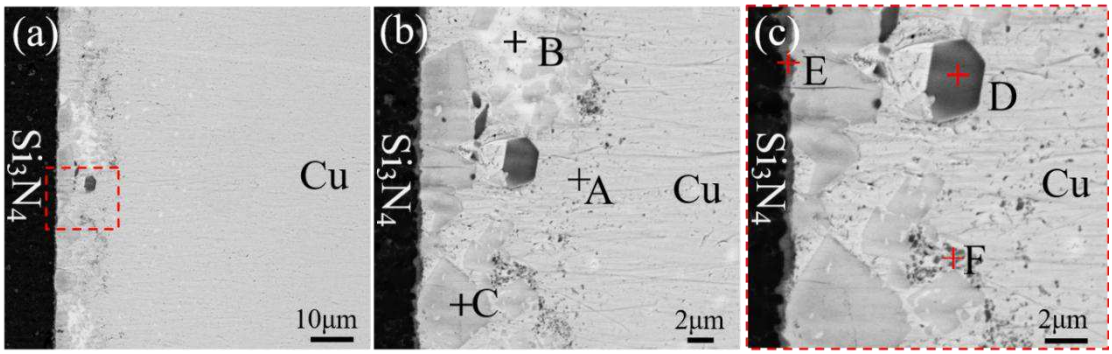


Fig.4 Microstructure of Si_3N_4/CuSnTi/Cu joint brazed with CuSnTi filler metal at 900 ℃-20 min.

Table 1 Analysis of points marked in Fig.4 (at.%).

	Sn	Cu	Ti	N	Si	Possible phase
A	2.68	95.80	0.54	0.06	0.92	Cu(s,s)
B	26.78	14.70	55.43	0.04	3.05	Sn_3Ti_5
C	8.88	40.35	45.98	0.25	4.54	CuTi
D	2.2	5.54	57.09	0.24	34.93	Ti_5Si_3
E	0.46	12.65	35.98	33.96	16.95	TiN
F	1.93	73.18	23.88	0.06	0.95	$CuTi_2$+Cu(s,s)

$$5Ti(l) + 3Si(s) = Ti_5Si_3 \ \ \Delta G\ (KJ/mol) = -194 + 0.0167T \quad (2)$$

$$Si_3N_4(s) + 3Ti(s) = 4TiN(s) + 3Si(s) \ \ \Delta G\ (KJ/mol) = -1356 + 0.199T \quad (3)$$

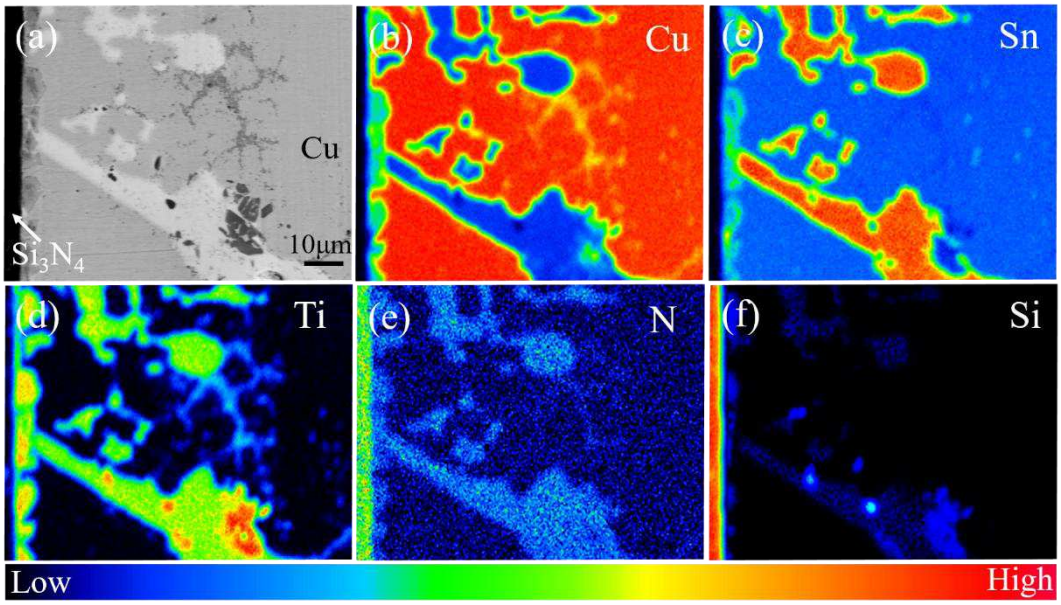


Fig.5 Microstructure and element distribution of Si_3N_4/CuSnTi/Cu joint.

The fracture surface on the Cu side after peeling was characterized by XRD, and the corresponding pattern is displayed in Fig.6. The results confirm the existence of TiN, Cu, Si_3N_4, Ti_5Si_3, Sn_3Ti_5, and $CuTi_2$ phases. In agreement with the above analysis, the Sn_3Ti_5 phase is identified in the fracture, whereas no other Sn-containing phases are observed in Fig.4. According to previous reports [32,33], the phase at point B in Table 1 is usually identified as either $CuSn_3Ti_5$ or Sn_3Ti_5. Jiang et al. [32] investigated the Cu-Sn-Ti ternary system via experiments and thermodynamic calculations, and verified that the $CuSn_3Ti_5$ phase is actually the binary intermetallic compound Sn_3Ti_5 with a certain solid solubility of Cu. On the basis of the above results, the typical interfacial microstructure of the Si_3N_4/Cu joint brazed with CuSnTi filler can be determined as: Si_3N_4/TiN+Ti_5Si_3+Cu(s，s)+CuTi+$CuTi_2$+Sn_3Ti_5/Cu.

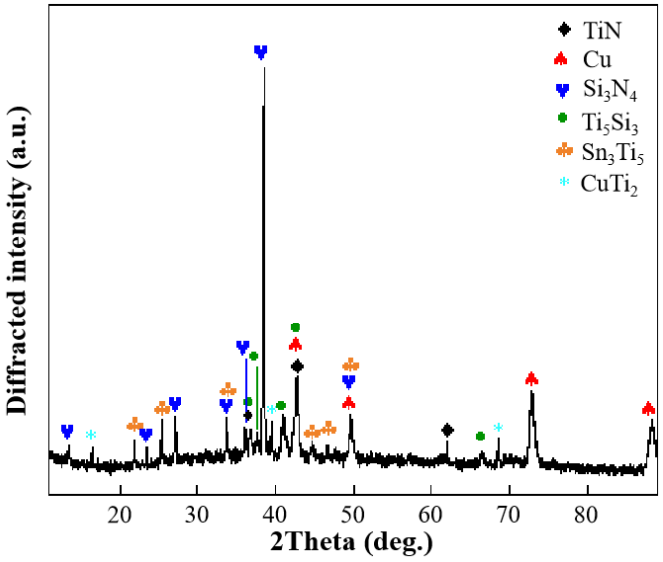


Fig.6 XRD pattern of Cu side after peeling.

3.2. Influence of brazing temperature on the microstructure and mechanical properties of Si_3N_4/CuSnTi/Cu joints

To investigate the effect of brazing temperature on the interfacial microstructure of Si_3N_4/Cu joints, vacuum brazing was carried out using CuSnTi filler at 850-1000 °C with a holding time of 20 min. The microstructure of the as-brazed joints is presented in Fig.7. At 850 °C, the molten filler shows insufficient fluidity, resulting in inadequate filling of the joint gap. Numerous voids are formed, and only a small amount of filler is squeezed out under low pressure, leading to a relatively wide brazing seam. The low element diffusion coefficient restricts the diffusion of Ti toward the Si_3N_4 substrate, leading to a thinner TiN reaction layer and less release of Si atoms. Consequently, no free Ti_5Si_3 phase is observed in the joint. Instead, most Ti atoms remain in the brazing seam and react with Sn to form white Sn_3Ti_5 particles, which are uniformly distributed in the joint (Fig.7a).

With increasing brazing temperature, the fluidity of the molten filler is gradually improved. Sound bonding is achieved at 900-1000 °C. Meanwhile, the amount of overflowed liquid filler increases under low pressure, and the brazing seam width is gradually reduced, accompanied by a decrease in the amount of white Sn_3Ti_5 phase. The elevated temperature enhances the element activity and accelerates the diffusion rate of Ti, promoting the migration of more Ti atoms to the ceramic side to form a TiN reaction layer. As observed in the magnified images (Fig. 7b-d), the thickness of the TiN layer increases gradually with temperature, reaching approximately 0.5 μm at 1000 °C. The thickened TiN layer also promotes the release of more Si atoms from Si_3N_4, which diffuse across the reaction layer and react with Ti to form free Ti_5Si_3 phase. At 900 °C, a small amount of hexagonal Ti_5Si_3 is formed in the joint. As the temperature

rises to 950 °C, the amount of black Ti_5Si_3 increases significantly. When the temperature reaches 1000 °C, coarsened Ti_5Si_3 grains are observed. Fine Ti_5Si_3 grains possess lower thermodynamic stability and higher surface energy. According to the literature [34], fine Ti_5Si_3 grains tend to dissolve and re-precipitate onto coarse grains to minimize the total surface energy. Therefore, with increasing brazing temperature, the number of Ti_5Si_3 grains decreases gradually while the grain size increases significantly. In addition, large blocky CuTi and a small amount of dispersed $CuTi_2$ are formed at 900 °C. When the temperature is increased to 950 and 1000 °C, the blocky CuTi phase disappears, while the amount of dispersed $CuTi_2$ increases.

At 850 °C, no effective bonding is established at the interface, and the Cu foil peels off directly from the ceramic substrate. Fig. 8 shows the peel strength of Si_3N_4/Cu joints brazed with CuSnTi filler at 900-1000 °C. The peel strength increases continuously with increasing temperature and reaches the maximum value of 32.1 N/mm at 1000 °C.

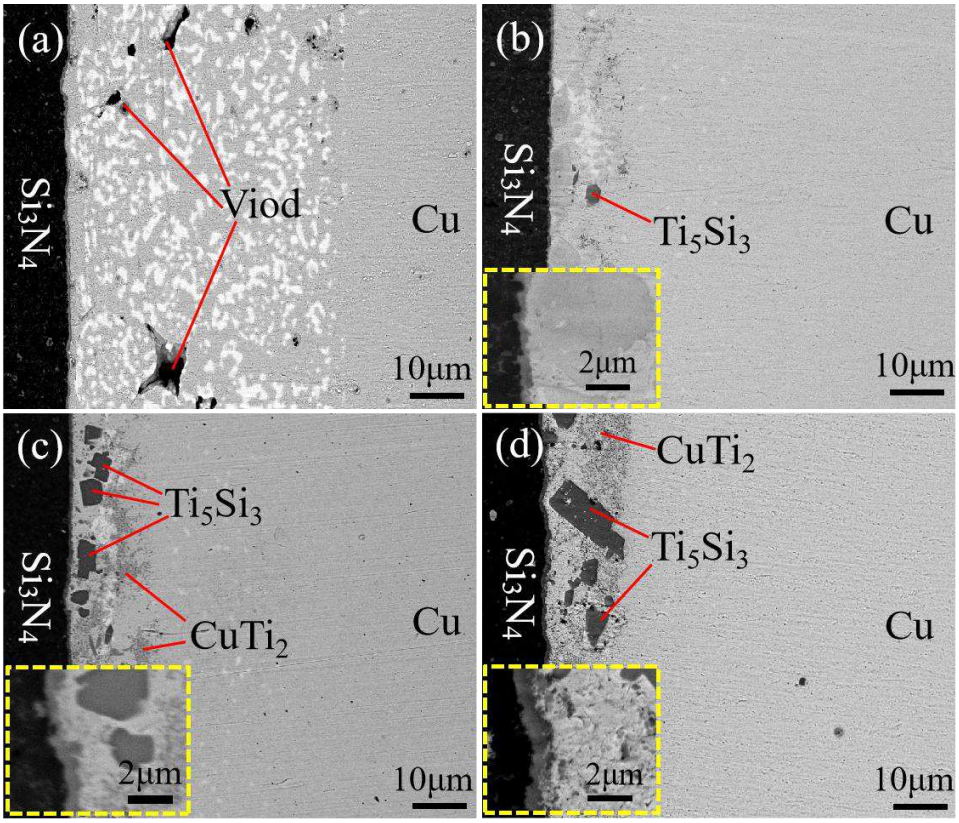


Fig.7 Microstructure of Si_3N_4/CuSnTi/Cu joint at different temperature: a 850 ℃; b 900 ℃; c 950 ℃; d 1000 ℃.

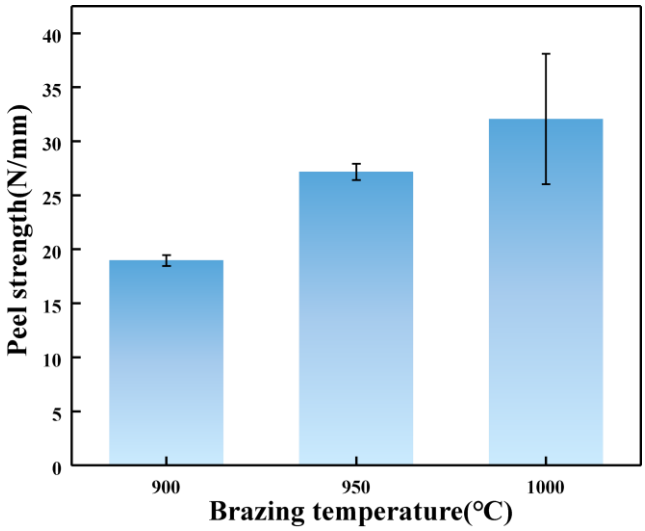


Fig.8 Peeling strength of Si_3N_4/CuSnTi/Cu joints at different temperatures.

The mechanical properties of the joint are significantly dominated by the phase composition and distribution within the joint. The coefficients of thermal expansion (CTE) of typical phases in the Si_3N_4/Cu joint are listed in Table 2. Figure 9 shows the

fracture morphologies on the Cu side of Si_3N_4/CuSnTi/Cu joints brazed at different temperatures. At a brazing temperature of 900 °C, a large amount of black Si_3N_4 ceramic phase and a small quantity of white brazing alloy structure can be observed on the fracture surface (Fig.9a, d), and the corresponding peel strength is 18.9 N/mm. At 900 °C, the activity of Ti in the brazing filler is relatively low, leading to a thin reaction layer formed at the ceramic interface. More Ti atoms remain in the brazing seam to form blocky CuTi phase, which is unevenly distributed in the joint. Under external loading, cracks initiate and propagate on the ceramic surface and inside the ceramic, resulting in brittle fracture. When the brazing temperature is increased to 950 °C and 1000 °C, a large number of Ti_5Si_3 phases are generated in the joint. The joint structure evolves from Si_3N_4/thin TiN layer/brazing alloy to Si_3N_4/thin TiN layer/rod-like Ti_5Si_3 phase/brazing alloy. The CTE mismatch between the transitional layers is gradually reduced, which relieves the residual stress in the joint and thus improves the joint strength. As observed in Fig.9, the area fraction of white brazing alloy structure on the fracture surfaces increases gradually at 950 °C and 1000 °C, demonstrating that the residual stress within the joint has been effectively relaxed.

Table 2 CTE of different components in the joint.

Material	CTE/（$\times 10^{-6}$ K^{-1}）
Si_3N_4	3.2
TiN	8.5
Ti_5Si_3	7.1
Cu	17.0

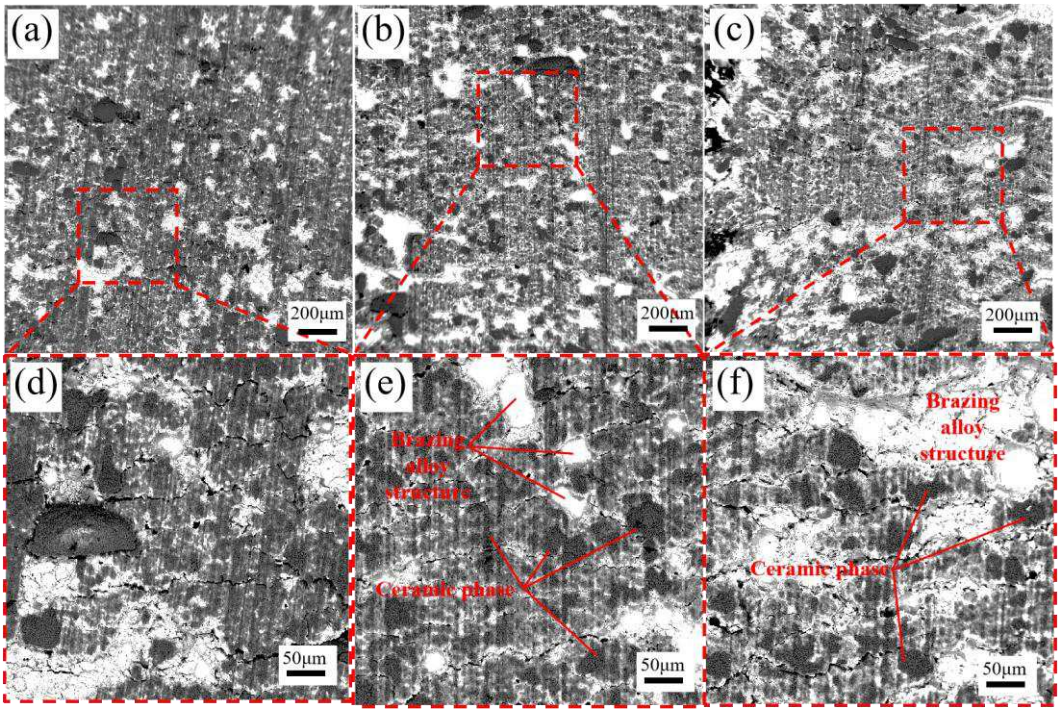


Fig.9 Cu side peeling fracture of Si_3N_4/CuSnTi/Cu joint at different brazing temperatures: a 900 ℃; b 950 ℃; c 1000 ℃; d-f enlarged image of the fracture.

3.3 Effect of In Addition on the Microstructure and Mechanical Properties of Si_3N_4/CuSnTi/Cu Joints

In the previous section, Si_3N_4/Cu joints were successfully brazed using CuSnTi filler, and the optimal brazing temperature was determined to be 1000 °C. For conventional CuTi brazing fillers, the typical brazing temperature is generally around 1000 °C [35,36]. Although the addition of Sn effectively reduces the melting point of the filler, the brazing temperature is still relatively high for industrial applications. Therefore, the low-melting-point element In was introduced into the CuSnTi filler, and the influences of brazing temperature on the interfacial microstructure and peel strength of the joints were studied.

Figure 10 shows the interfacial microstructure of the Si_3N_4/Cu joint brazed with CuInSnTi filler (CuSnTi+10 wt.% In) at 900 °C for 20 min. The joint exhibits sound

bonding without noticeable defects such as voids or cracks. A magnified view of the brazing layer (Fig.10b) reveals no obvious new phases compared with the CuSnTi brazed joint. The brazing seam mainly consists of a large amount of white phase A, a small quantity of black blocky phase B, and dark gray blocky phase C. Further magnification of the ceramic-side reaction layer (Fig.10c) shows a distinct reaction layer phase D, together with dispersed black phase E distributed in the brazing seam. To identify the phase constituents after In addition, quantitative compositional analysis was conducted on phases A–E by EDS, and the results are listed in Table 3. The In content in all these phases is relatively low. Combined with the previous analysis, these phases are identified as Sn_3Ti_5, Ti_5Si_3, CuTi, TiN, and $CuTi_2$, respectively.

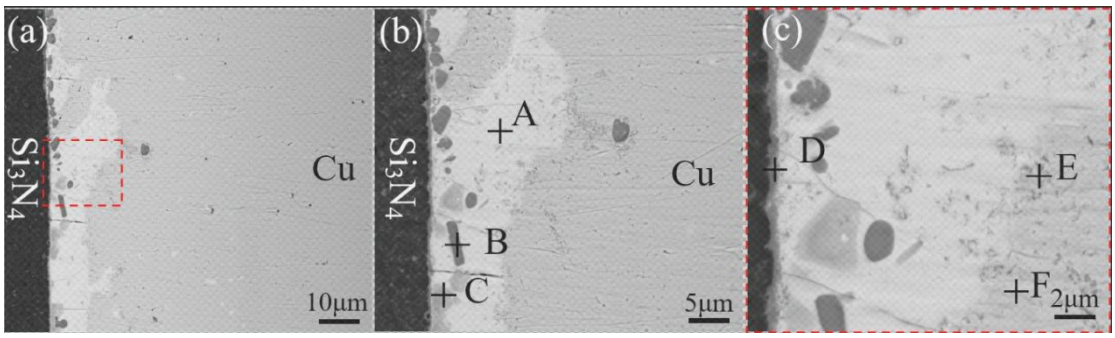


Fig.10 Microstructure of Si_3N_4/Cu joint brazed with CuInSnTi brazing metal at 900 ℃-20 min: a whole joint; b-c partial enlarged image.

Table 3 Analysis of points marked in Fig.10 (at.%).

	Si	Sn	N	Cu	In	Ti	Possible phase
A	3.32	25.86	0.04	16.34	0.56	53.88	Sn_3Ti_5
B	33.05	1.25	3.07	2.16	0.05	60.42	Ti_5Si_3
C	6.25	10.99	0.04	32.52	0.60	49.60	CuTi
D	15.49	0.74	32.30	5.56	0.38	45.53	TiN
E	0.95	1.73	0.06	73.17	2.21	21.88	Cu(s,s)+$CuTi_2$
F	1.34	2.37	0.04	88.74	6.73	0.78	Cu(s,s)

Phase F is mainly composed of 88.74 at.% Cu and 6.73 at.% In. Besides, the In content in other phases within the brazed joint is quite low. Over the past few decades, extensive research has been carried out on the phase diagram and thermodynamics of the Cu-In binary system. It has been confirmed that the maximum solid solubility of In in Cu is 10.85 at.%, and the solid solubility gradually decreases with the decrease of brazing temperature. However, studies on Cu-In alloys with low In content are relatively scarce. Considering the high vapor pressure of metallic In, it tends to volatilize during vacuum brazing. Meanwhile, existing as a solid solution can significantly reduce its volatilization rate. According to the Cu–In phase diagram [37], In exhibits higher solid solubility in the Cu matrix than other elements during brazing, and the holding time at high temperature is relatively short. Therefore, the volatilization of In is neglected in this work. In terms of atomic radius, the radius of Cu is 1.28 Å while that of In is 1.62 Å. The large difference in atomic radius exceeds 15%, which violates the Hume-Rothery rule, leading to low solid solubility at room temperature [38]. Elemental mapping of Cu, In, and Sn in the joint was performed by EPMA, as presented in Fig.11. A corresponding distribution between Cu and In can be observed. At a distance of 40 μm from the ceramic interface, the signal intensity of In gradually decreases with increasing distance from the interface. EPMA line scan was also conducted along the path shown in Fig. 11, and the results are displayed in Fig. 12. The In content exhibits a linear decreasing trend with increasing distance from the brazing seam. Based on the above analysis, it is inferred that after adding In into the filler, In dissolves into the Cu matrix at high temperatures, which lowers the melting point of

the brazing alloy. Meanwhile, In diffuses toward the Cu substrate driven by the chemical potential gradient. During the slow furnace cooling process, the solid solubility of In in the Cu matrix decreases continuously, resulting in the precipitation of a small amount of δ phase in the joint. Finally, a mixture of δ phase and Cu-based solid solution is formed. Therefore, the typical interfacial microstructure of the Si_3N_4/CuInSnTi/Cu brazed joint can be described as:Si_3N_4/TiN+Ti_5Si_3+Cu(s, s)+CuTi+$CuTi_2$+Sn_3Ti_5/Cu.

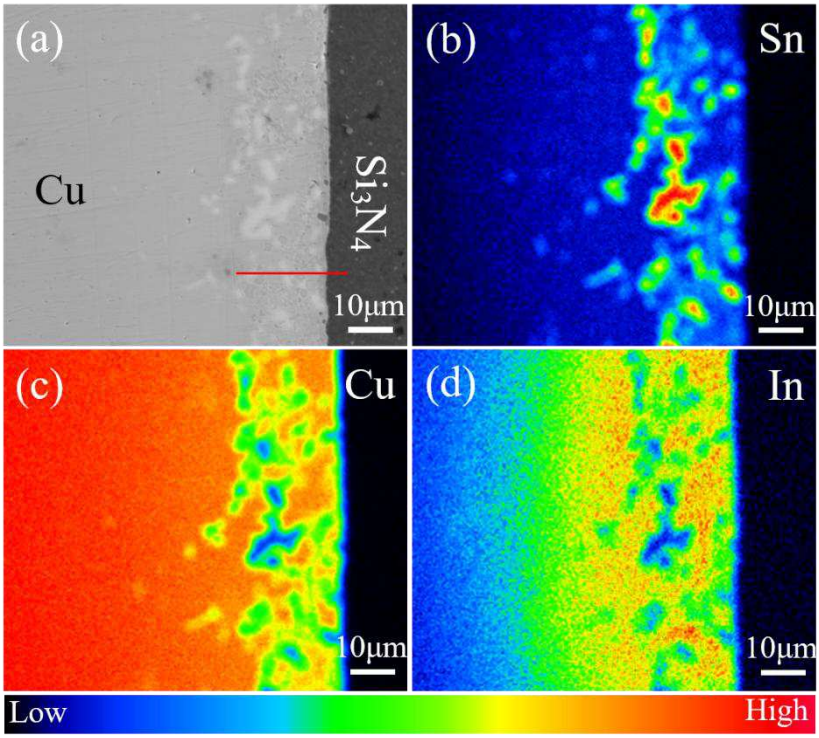


Fig.11 Microstructure and element distribution of Si_3N_4/CuInSnTi/Cu joint.

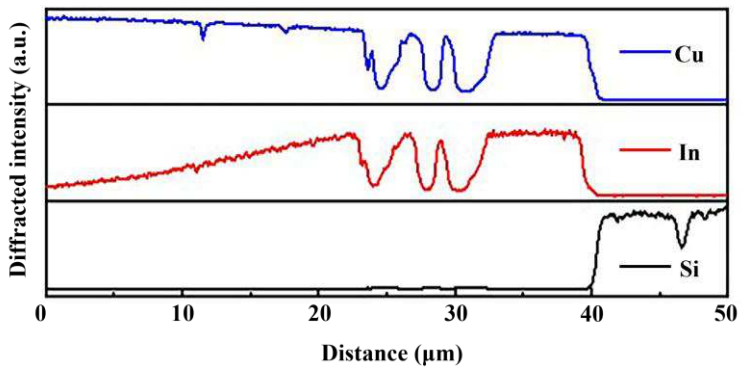


Fig.12 EDS line profiles of the elements of Figure 11(a).

To investigate the influence of In addition on the melting point and brazability of the filler metal, Si_3N_4/Cu joints were brazed using CuInSnTi filler at various temperatures. The interfacial microstructure of the joints is presented in Fig.13. At relatively low brazing temperatures, the fluidity of the molten filler is insufficient, resulting in a large number of void defects in the joint. With increasing brazing temperature, the fluidity of the brazing alloy is gradually enhanced, and more liquid filler is extruded from the brazing layer under applied pressure, leading to a gradual reduction in the brazing seam width. Sound interfacial bonding is achieved at 850-900 °C without any defects such as voids or cracks. The increase in brazing temperature accelerates elemental diffusion. At low temperatures, the white Sn-containing phase in the brazing seam is uniformly distributed as blocky particles. When the temperature rises to 900 °C, the white phase aggregates and coarsens. Meanwhile, the activity of Ti is gradually improved, and more Ti atoms diffuse toward the ceramic side to form a thicker reaction layer, which promotes the release of more Si atoms. At 850 °C, a small amount of free black Ti_5Si_3 phase is observed in the joint. When the brazing temperature is increased to 900 °C, a large number of free Ti_5Si_3 phases appear near the ceramic interface.

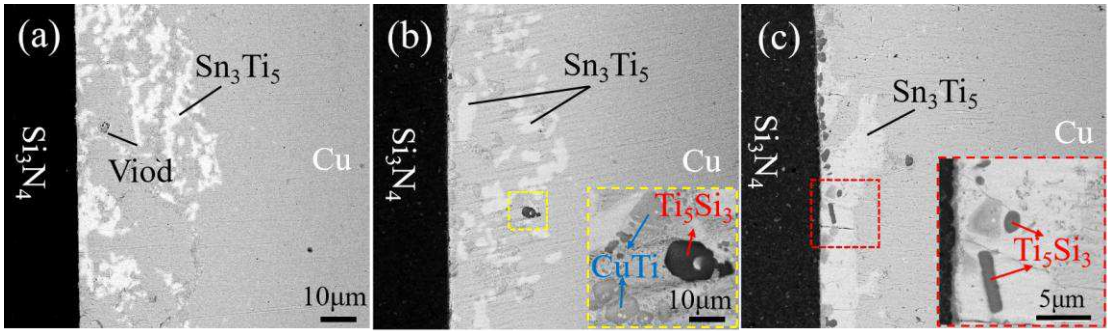


Fig.13 Microstructure of Si_3N_4/CuInSnTi/Cu joint at different temperatures:

a 820 ℃; b 850 ℃; c 900 ℃.

Figure 14 shows the peel strength of Si_3N_4/Cu joints brazed with CuInSnTi filler at 820-900 °C for a holding time of 20 min. The joint strength first increases and then decreases with increasing brazing temperature, reaching a maximum value of 20.58 N/mm at 850 °C.

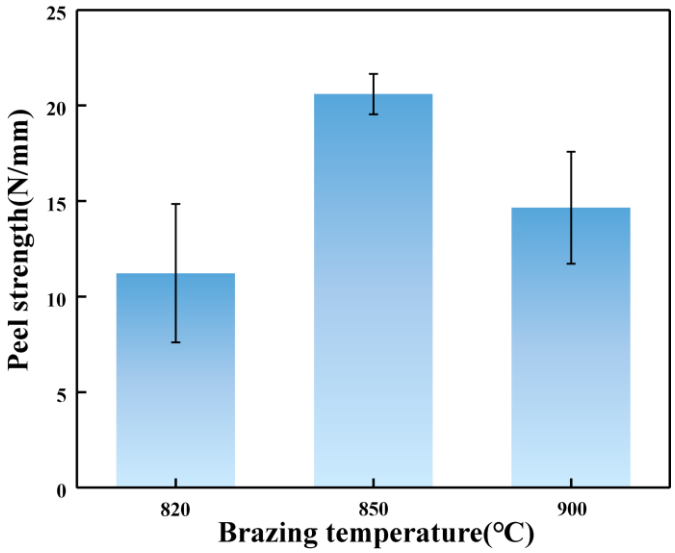


Fig.14 Peeling strength of Si_3N_4/CuInSnTi/Cu joints at different temperatures.

Figure 15 displays the fracture morphologies of the peeled joints obtained at different brazing parameters. At a brazing temperature of 820 °C, the activity of Ti in the brazing layer is relatively low, leading to a thin TiN reaction layer at the ceramic interface. Meanwhile, a large number of defects such as pores and cracks exist in the joint. Under external loading, fracture initiates at the defects within the ceramic surface layer and the brazing seam, resulting in a low peel strength of only 11.16 N/mm. With increasing brazing temperature, the thickness of the TiN reaction layer is increased and the fluidity of the brazing alloy is significantly improved, which effectively reduces the defects in the joint. Consequently, the peel strength is enhanced and the fracture surface becomes relatively flat, with failure occurring in the ceramic surface layer and inside

the brazing alloy. However, the residual stress in the joint also increases gradually with the elevation of brazing temperature. The amount of low-CTE Ti_5Si_3 phase formed in the joint is limited, leading to an insufficient effect on residual stress relaxation. When the brazing temperature reaches 900 °C, a small amount of large black Si_3N_4 ceramic phase is observed on the fracture surface. Under applied loading, cracks propagate along the defects into the deep region of the ceramic, causing the peel strength to decrease to 14.60 N/mm.

A comparison between the two fillers (with and without In addition) was carried out at 850 °C. In the case of CuSnTi filler without In, the filler shows poor fluidity at this temperature, resulting in numerous voids and eventual joint failure. After the addition of 10 wt.% In, In dissolves into the Cu matrix at high temperatures, which effectively reduces the melting point and improves the fluidity of the brazing alloy. This contributes to sound bonding of the joint, together with enhanced elemental activity and increased thickness of the ceramic-side reaction layer. Under the experimental conditions of this work, the optimal brazing temperature for the In-added CuInSnTi filler is determined to be 850 °C. Although the maximum peel strength is slightly lower than that of the CuSnTi joint, it is still much higher than the industrial requirement of 10 N/mm [39].

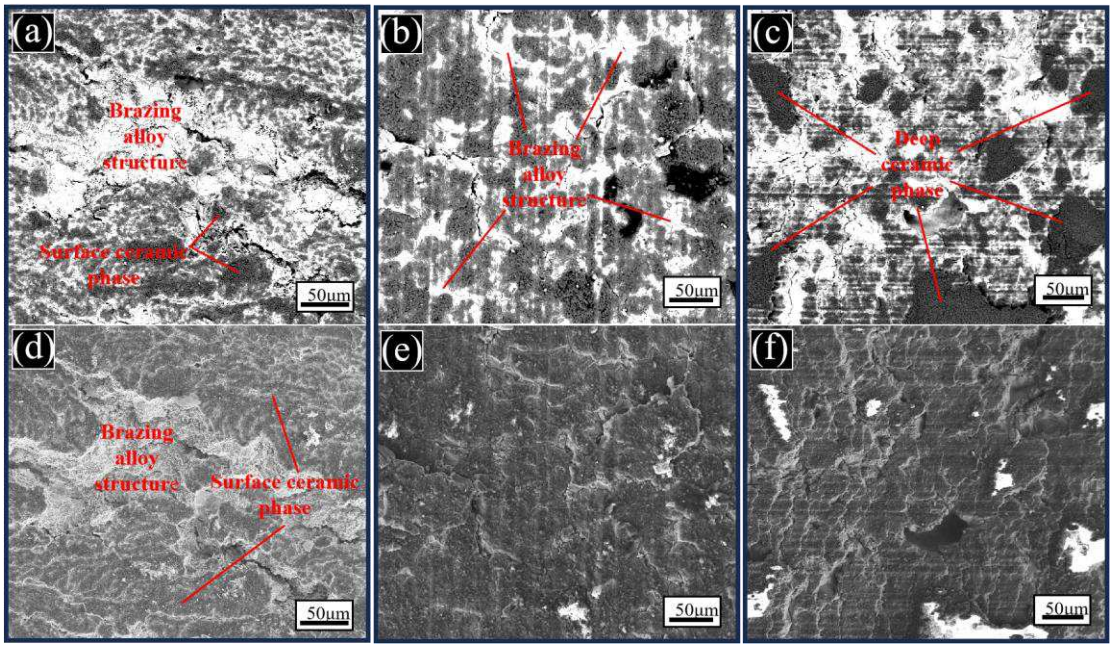


Fig.15 Peel fracture of Cu/CuInSnTi/Si_3N_4 joint at different brazing temperatures: a 850 ℃;b 900 ℃; c 950 ℃; d 850 ℃; e 900 ℃; f 950 ℃.

3.4 Microstructural evolution of Si_3N_4/CuSnTi/Cu joint

Based on the above analysis, the microstructural evolution mechanism of Si_3N_4/Cu joints brazed with CuSnTi and In-alloyed CuSnTi fillers is proposed. Fig.16(a-d) schematically illustrates the microstructural evolution of the joint brazed with CuSnTi filler, which can be divided into the following stages:

(1) With the gradual increase of brazing temperature, the brazing filler melts into liquid, which significantly accelerates the elemental diffusion in the joint.

(2) Driven by the chemical potential gradient, active Ti in the filler diffuses toward and accumulates at the Si_3N_4 ceramic side, while the Cu substrate starts to dissolve into the liquid filler.

(3) Interfacial chemical reactions take place in the joint. With the proceeding of brazing, Ti reacts with Si_3N_4 to form a continuous TiN reaction layer, accompanied by the release of Si atoms. The Si atoms diffuse across the TiN layer and react with Ti to

form the Ti_5Si_3 phase. Meanwhile, Cu from the substrate further dissolves into the brazing seam.

(4) The continuous interfacial reaction consumes Ti atoms, resulting in a reinforced chemical potential difference in the joint. This promotes the continuous diffusion of Ti from the filler to the ceramic interface, further thickening the TiN layer and releasing more Si atoms. Abundant large rod-like Ti_5Si_3 grains are generated and randomly distributed in the joint. Subsequently, with the decrease of brazing temperature, the solubility of elements in the liquid filler declines, leading to the formation and precipitation of Sn_3Ti_5, CuTi, $CuTi_2$ and other compounds, which finally solidify into the morphology shown in Fig. 16(d).

Fig.16(e–h) shows the microstructural evolution of Si_3N_4/Cu joints after In addition. With increasing temperature, In melts and dissolves into the Cu matrix, which reduces the melting point and improves the fluidity of the brazing alloy, enhances the activity of Ti, and thus promotes the thickening of the ceramic-side reaction layer. At high temperatures, In diffuses into the Cu substrate driven by the chemical potential gradient. During the subsequent furnace cooling, In precipitates from the Cu matrix in the form of Cu(In) solid solution and related compounds.

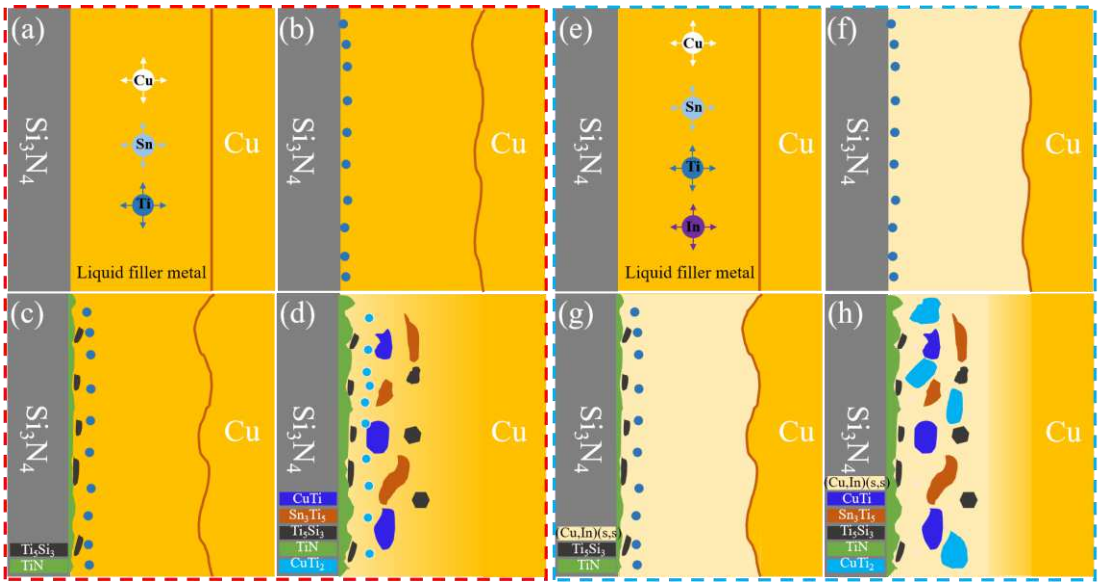


Fig.16 Microstructure evolution of Si_3N_4/Cu joint brazed with CuInSnTi filler metal: a-d CuSnTi brazing metal; e-h CuInSnTi brazing metal.

4. Conclusion

In this work, Si_3N_4 ceramic and Cu were successfully joined using CuSnTi active brazing filler. The typical interfacial microstructure of the Si_3N_4/Cu joint is identified as: Si_3N_4/TiN+Ti_5Si_3+Cu(s,s)+Sn_3Ti_5+CuTi+$CuTi_2$/Cu. With increasing brazing temperature, the activity of Ti is significantly enhanced, and more Ti atoms diffuse toward the ceramic side. The thickness of the TiN reaction layer increases gradually, and the amount of Ti_5Si_3 phase increases with an obvious tendency of aggregation and coarsening. Owing to the low coefficient of thermal expansion (CTE), Ti_5Si_3 acts as a transitional phase distributed in the joint and effectively relieves the residual stress. Consequently, the peel strength of the joint increases gradually with rising temperature and reaches a maximum value of 32.1 N/mm at 1000 °C. After the addition of In, the melting point of the brazing alloy is reduced, and both the fluidity of the liquid filler and the elemental activity are improved. Reliable Si_3N_4/Cu joints are obtained at 850 °C, with a peel strength of 20.58 N/mm. The addition of In shows negligible influence on

the phase composition of the joint. In is mainly solid-dissolved in the Cu matrix and precipitates as a mixture of Cu-based solid solution and related compounds during furnace cooling.

Funding

This research was sponsored by the Natural Science Foundation of Hebei Province (Grant Number E2021202177).

References

[1] R.Y. Wang, T.Y. Qin, Y.J. Shang, M.X. Wang, E.Z. Li, C.W. Zhong, Rapid preparation of Si_3N_4 ceramics with high thermal conductivity and low dielectric loss by fast hot-pressing (FHP) sintering. Ceram. Int. 50, 38550–38561 (2024) https://doi.org/10.1016/j.ceramint.2024.07.223

[2] C.P. Yang, Q. Liu, B. Zhang, J.J. Ding, Y.C. Jin, F. Ye, Z.G. Zhang, L.F. Gao, Effect of MgF_2 addition on mechanical properties and thermal conductivity of silicon nitride ceramics. Ceram. Int. 45, 12757–12763 (2019) https://doi.org/10.1016/j.ceramint.2019.03.183

[3] T. Lu, T. Wang, Y.F. Jia, M.M. Ding, Y. Shi, J.J. Xie, F. Lei, L. Zhang, L.C. Fan, Fabrication of high thermal conductivity silicon nitride ceramics by pressureless sintering with MgO and Y_2O_3 as sintering additives. Ceram. Int. 46, 27175–27183 (2020) https://doi.org/10.1016/j.ceramint.2020.07.198

[4] W. Yao, B. Zhong, Y.M. Zhang, Y.F. Zhou, H.T. Wang, F. Shi, Effects of brazing parameters on interfacial reaction layer characteristics and mechanical performance of brazed Cu/Si_3N_4 using Ag-Cu-Ti filler alloy. Mater. Sci. Eng. A-Struct. Mater. Prop. Microstruct. Process. 936, 148400 (2025) https://doi.org/10.1016/j.msea.2025.148400

[5] X.L. Wu, C.Y. Li, J.L. Yang, Y. Liu, X.H. Han, Theoretical and experimental research on flow boiling heat transfer in microchannels for IGBT modules. Int. J. Heat Mass Transf. 205, 123900 (2023) https://doi.org/10.1016/j.ijheatmasstransfer.2023.123900

[6] F. Mohammadi, S.S. Li, Copper like thermal conductivity and silicon like coefficient of thermal expansion copper graphene for high power IGBT by metal injection molding. Mater. Trans. 59, 1677–1683 (2018) https://doi.org/10.2320/matertrans.M2018136

[7] L.P. Tan, P.S. Liu, C.H. She, P.P. Xu, L. Yan, H. Quan, Heat dissipation characteristics of IGBT module based on flow-solid coupling. Micromach. 13, 554 (2022) https://doi.org/10.3390/mi13040554

[8] A. Fukumoto, D. Berry, K.D.T. Ngo, G.Q. Lu, Effects of extreme temperature swings (-55℃ to 250℃) on silicon nitride active metal brazing substrates. IEEE Trans. Device Mater. Rel. 14, 751–756 (2014) https://doi.org/10.1109/TDMR.2014.2320057

[9] S.W. Sun, T. Wang, Z.L. Yu, W.B. Guo, X.G. Chen, Microstructure and mechanical properties of AlN and Cu joint using SnAgTi solder metal. J. Mater. Sci. Mater. Electron. 35, 1516 (2024) https://doi.org/10.1007/s10854-024-13276-y

[10] M. Li, K.Q. Shi, D.D. Zhu, D. Dong, L. Liu, X.H. Wang, Microstructure and mechanical properties of Si_3N_4 ceramic and ($TiB+Y_2O_3$)/Ti matrix composite joints brazed with AgCu/Cu foam/AgCu multilayered filler. J. Manuf. Process. 66, 220–227 (2021) https://doi.org/10.1016/j.jmapro.2021.04.025

[11] Z.W. Yang, M.M. Fang, Z. Yong, Q. Wen, S.Y. Niu, Y. Wang, Enhanced properties in Si_3N_4/Cu AMB joints through regulating interfacial reaction modes induced by Mo-particle additives. Ceram. Int. 50, 43969–43978 (2024) https://doi.org/10.1016/j.ceramint.2024.08.248

[12] X.G. Song, Y.X. Zhao, S.P. Hu, J. Cao, W. Fu, J.C. Feng, Wetting of AgCu–Ti filler on porous Si_3N_4 ceramic and brazing of the ceramic to TiAl alloy. Ceram. Int. 44, 4622–4629 (2018) https://doi.org/10.1016/j.ceramint.2017.11.212

[13] J. Zhang, J.P. Xu, J. Huang, R.X. Liu, Y. Xiao, G.Q. Luo, High shear strength Kovar/AlN joints brazed with AgCuTi/Cu/AgCuTi sandwich composite filler. Mater. Sci. Eng. A 862, 144435 (2023) https://doi.org/10.1016/j.msea.2022.144435

[14] J. J. Wang, Negative thermal expansion of $LiAlSiO_4$ interlayer with AgCuTi filler for brazing SiC joints. Int. J. Appl. Ceram. Technol. 22, e15045 (2025) https://doi.org/10.1111/ijac.15045

[15] Z.R. Chen, X.J. Liu, Z.Q. Zhang, Enhancement of joint properties in B_4C/TC4 connections by adding AlN to AgCuTi brazing materials. Philos. Mag. 105, 698–715 (2025) https://doi.org/10.1080/14786435.2025.2451076

[16] L. L. Tang, D. X. Yao, Y. F. Xia, H. Q. Liang, Y.-P. Zeng, Effect of interfacial microstructure evolution on the peeling strength and fracture of silicon nitride/oxygen-free copper foil joints brazed with Ag-Cu-TiH_2 filler. J. Eur. Ceram. Soc. 43, 4374–4385 (2023) https://doi.org/10.1016/j.jeurceramsoc.2023.03.038

[17] L.L. Yuan, W. Wang, X.M. Huang, Y.F. Qi, X.Y. Li, Joining of Al_2O_3 to Cu with Cu-Sn-Ti active brazing filler alloy. Weld. World 66, 1471–1479 (2022) https://doi.org/10.1007/s40194-022-01305-5

[18] S. Buhl, C. Leinenbach, R. Spolenak, K. Wegener, Microstructure, residual stresses and shear strength of diamond–steel joints brazed with a Cu–Sn-based active filler alloy. Int. J. Refract. Met. Hard 30, 16–24 (2012) https://doi.org/10.1016/j.ijrmhm.2011.06.006

[19] F. Habibi, A. Samadi, Interfacial reactions in actively brazed Cu-Al_2O_3 composites and copper using a newly developed Cu-Sn-Ag-Ti filler alloy. Sci. Technol. Weld. Join. 28, 444–454 (2023) https://doi.org/10.1080/13621718.2023.2173878

[20] M. Naka, I. Ono, Wetting of silicon nitride by copper–titanium or copper–zirconium alloys. Trans. JWRI 14, 29-34 (1985) https://doi.org/10.1115/1.3426897

[21] L. Wang, Q.L. Lin, R. Sui, Effect of Ti concentration on the wetting of molten Cu-8.6Zr-xTi alloys on Si_3N_4 substrate. Surf. Interf. 31, 102076 (2022) https://doi.org/10.1016/j.surfin.2022.102076

[22] W.H. Liu, P.C. Wang, W.T. Shi, S. Zhao, X. Nai, X.G. Song, H.Y. Chen, W.Y. Li, Investigating the effect of WC reinforcements in Cu–Ti composite filler on the microstructural evolution and mechanical characteristics in brazing C_p/SiC and GH3536. J. Manuf. Process. 121, 312–322 (2024) https://doi.org/10.1016/j.jmapro.2024.05.051

[23] S.X. Liu, B. Xiao, Z.Y. Zhang, D.Z. Duan, Microstructural characterization of diamond/CBN grains steel braze joint interface using Cu-Sn-Ti active filler alloy. Int. J. Refract. Met. Hard 54, 54–59 (2016) https://doi.org/10.1016/j.ijrmhm.2015.07.008

[24] Q.B. Du, X. Liu, B. Cui, L.X. Qu, A. Li, Z.Y. Min, Q. Yang, A first-principles study on the interfacial behavior of Cu-Sn-Ti brazing alloys with diamond and the effects of Fe, Cr, and Si doping. Diam. Relat. Mater. 161, 113164 (2026) https://doi.org/10.1016/j.diamond.2025.113164

[25] B. Cui, Z.W. Liu, Q.B. Du, H.L. Deng, L. Yang, Exploring the role of indium on the microstructure evolution and interface bonding behavior of brazing diamond abrasive with modified Cu-Sn-Ti. Diam. Relat. Mater. 136, 110068 (2023) https://doi.org/10.1016/j.diamond.2023.110068

[26] S.H. Rajendran, S.J. Hwang, J.P. Jung, Active brazing of alumina and copper with multicomponent Ag–Cu–Sn–Zr–Ti filler. Metals 11, 509 (2021) https://doi.org/10.3390/met11030509

[27] S.S. Guo, L.B. Sun, J. Fang, Z. Zheng, J. Zhang, Y. Wen, T.P. Shan, C.F. Liu, Residual stress, microstructure and corrosion behavior in the 316L/Si_3N_4 joint by multi-layered braze structure-experiments and simulation. Ceram. Int. 48, 32894–32907 (2022) https://doi.org/10.1016/j.ceramint.2022.07.218

[28] M. Singh, J.M. Fernandez, R. Asthana, J. Ramirez Rico, Interfacial characterization of silicon nitride/silicon nitride joints brazed using Cu-base active metal interlayers. Ceram. Int. 38, 2793–2802 (2012) https://doi.org/10.1016/j.ceramint.2011.11.050

[29] C. Zhou, Research on joining process of Si_3N_4 and 316L stainless steel. Zhenjiang: Jiangsu University of Science and Technology (2021) https://doi.org/2019. 10.27171/d.cnki.ghdcc.2019.000336

[30] W. Guo, H.Q. Zhang, K.T. Ma, Y. Zhu, H. Zhang, B.J. Qi, F. Li, P. Peng, Reactive brazing of silicon nitride to Invar alloy using Ni foam and AgCuTi intermediate layers. Ceram. Int. 45, 13979–13987 (2019) https://doi.org/10.1016/j.ceramint.2019.04.097

[31] Y.X. Zhao, M.R. Wang, J. Cao, X.G. Song, D.Y. Tang, J.C. Feng, Brazing TC4 alloy to Si_3N_4 ceramic using nano-Si3N4 reinforced AgCu composite filler. Mater. Des. 76, 40–46 (2015) https://doi.org/10.1016/j.matdes.2015.03.046

[32] J. Wang, C. Liu, C. Leinenbach, U.E. Klotz, P.J. Uggowitzer, J.F. Löffler, Experimental investigation and thermodynamic assessment of the Cu–Sn–Ti ternary system. Calphad 35, 82–94 (2011) https://doi.org/10.1016/j.calphad.2010.12.006

[33] S.H. Wang, Z.Y. Zheng, Y.L. Li, A. Du, R.A. Ma, Y.Z. Fan, X. Zhao, X.M. Cao, Microstructure and properties of a YG18/40Cr joint vacuum-brazed by Cu-Sn-Ti filler metal. Vacuum 217, 112511 (2023) https://doi.org/10.1016/j.vacuum.2023.112511

[34] L.L. Tang, D.X. Yao, Y.F. Xia, H.Q. Liang, Y.P. Zeng, Effect of interfacial microstructure evolution on the peeling strength and fracture of silicon nitride/oxygen-free copper foil joints brazed with Ag–Cu–TiH_2 filler. J. Eur. Ceram. Soc. 43, 4374–4385 (2023) https://doi.org/10.1016/j.jeurceramsoc.2023.03.038

[35] Y.Q. Xia, H.G. Dong, X.H. Hao, P. Li, S. Li, Vacuum brazing of Ti6Al4V alloy to 316L stainless steel using a Ti–Cu-based amorphous filler metal. J. Mater. Process. Technol. 269, 35–44 (2019) https://doi.org/10.1016/j.jmatprotec.2019.01.020

[36] Y. Zhang, Y.K. Chen, D.S. Yu, D.Q. Sun, H.M. Li, A review on effect of the welding process of ceramics and metals. J. Mater. Res. Technol. 9(6), 16214–16236 (2020) https://doi.org/10.1016/j.jmrt.2020.11.088

[37] F.L. Chang, Y.H. Lin, H.T. Hung, C.R. Kao, Experimental and thermodynamic assessment of the Cu–In system. Calphad 85, 102700 (2024) https://doi.org/10.1016/j.calphad.2024.102700

[38] X. Ma, L.F. Zhang, Z.H. Zhang, H. Wang, E.Z. Wang, T. Qiu, Microstructure and melting properties of Ag-Cu-In intermediate-temperature brazing alloys. Rare Met. 34, 324–328 (2015) https://doi.org/10.1007/s12598-015-0484-7

[39] Y. Zhao, L.J. Liu, Y.G. Wu, et al., Research advances of silicon nitride ceramic AMB copper-clad substrates for SiC power modules. Micronanoelectronic. Technology. 61(8), 080001 (2024) https://doi.org/10.13250/j.cnki.wndz.24080001